NASA TECHNICAL MEMORANDUM

NASA TM-73862

NASA TM-73862

OPTIMUM WALL IMPEDANCE FOR SPINNING MODES - A CORRELATION WITH MODE CUT-OFF RATIO

by Edward J. Rice
Lewis Research Center
Cleveland, Ohio 44135

TECHNICAL PAPER to be presented at the
Sixteenth Aerospace Sciences Meeting
sponsored by the American Institute of Aeronautics and Astronautics
Huntsville, Alabama, January 16-18, 1978

OPTIMUM WALL IMPEDANCE FOR SPINNING MODES - A CORRELATION WITH MODE CUT-OFF RATIO

Edward J. Rice
National Aeronautics and Space Administration
Lewis Research Center
Cleveland, Ohio 44135

Abstract

A correlating equation relating the optimum acoustic impedance for the wall lining of a circular duct to the acoustic mode cut-off ratio is presented and compared to exact calculations. The optimum impedance was correlated with cut-off ratio because the cut-off ratio appears to be the fundamental parameter governing the propagation of sound in the duct. Modes with similar cut-off ratios respond in a similar way to the acoustic liner. The correlating equation is useful for the design of suppressors for aircraft engine inlets having a steady mean flow with a boundary layer and spinning mode noise source excitation. The correlation is a semi-empirical expression developed from an empirical modification of an equation originally derived from sound propagation theory in a thin boundary layer. Exact calculations of the optimum wall impedance were made over a wide range of frequency parameters, boundary layer thicknesses and flow Mach numbers to develop and verify the correlation. This correlating equation represents a part of a simplified liner design method, based upon modal cut-off ratio, for multimodal noise propagation.

Introduction

Spinning modes must be considered[1,2,3] in the design of acoustic suppressors with wall treatment only. With multimodal noise, as typically generated by a turbofan engine, the suppressor design will depend on the acoustic power distribution among the various modes. In some analyses assumptions of equal modal amplitude[4] and equal acoustic power per mode[1,5] have been used. Experimental measurement of the modal amplitudes and phases have also been attempted for quite simple modal structures in rectangular[6] and annular[7] ducts. However, it appears that if a large number of propagating modes are possible, direct measurement of these modes may be extremely difficult.[7]

In order to avoid the direct measurement of modes a simplified method of liner design based upon the acoustic power distribution as a function of mode cut-off ratio is under development. The philosophy of this simplified design method has been outlined in Ref. 8. It is based upon the fact that modes with similar cut-off ratios behave similarly in an acoustically lined duct. Similar maximum possible attenuations and similar optimum impedances[8,9] were observed for modes with a common cut-off ratio. The similarity of off-optimum performance can also be inferred from the approximate attenuation method of Ref. 10. A method for estimating the acoustic power-cutoff ratio distribution from far-field measurements has recently been reported.[11]

An essential ingredient in this simplified liner design approach is a correlation of optimum acoustic impedance as a function of mode cut-off ratio. A preliminary correlation based upon limited calculations was presented in Ref. 8. The purpose of this paper is to provide an improved correlation of optimum acoustic impedance based upon exact calculations of sound propagation in an acoustically lined duct using a wide range of the variables of frequency parameter, steady flow Mach number, and boundary layer thickness. Some of the pertinent development of the correlating equation is also included. A method for using this equation to obtain single mode optimum impedance estimates is also outlined.

Symbols

B_θ	optimum resistance coefficient
B_χ	optimum reactance coefficient
c	speed of sound, m/sec
D	duct diameter, m
F	refraction function, see equation (5)
f	frequency, Hz
G	empirical function, see equations (4), (13), and (14)
Q	$1 + M_o (J + i\tau)$
M_o	uniform steady flow Mach number in duct
m	spinning mode lobe number (circumferential order)
R	amplitude of eigenvalue α
R_m	value of R at the optimum impedance
$R_{m,\mu}$	R_m with modal indices included
r	radial coordinate, m
r_o	circular duct radius, m
x	axial coordinate, m
α	complex radial eigenvalue ($\alpha = Re^{i\varphi}$)
δ	boundary layer thickness for 1/7th power velocity profile, m
ϵ	dimensionless boundary layer thickness, δ/r_o
ζ	optimum specific acoustic impedance with a boundary layer
ζ_o	optimum specific acoustic impedance with zero boundary layer thickness (slip flow)
η	frequency parameter, fD/c
θ	specific acoustic resistance
θ_m	optimum specific acoustic resistance
θ_{mo}	θ_m with boundary layer neglected
μ	radial mode order
ξ	mode cut-off ratio, see equation (1)
σ	attenuation coefficient

τ propagation coefficient

θ angular coordinate, radians

φ phase of eigenvalue, degrees

φ_G phase of function G, see equation (14), degrees

$\Delta\varphi_G$ part of φ_G, see equations (15) and (16), degrees

φ_m phase of eigenvalue at optimum impedance, degrees

$\varphi_{m,\mu}$ φ_m with modal indices included

χ specific acoustic reactance

χ_m optimum specific acoustic reactance

χ_{mo} χ_m with boundary layer neglected

ω circular frequency, rad/sec

Sound Propagation Model

The sound propagation theory used for the so-called exact calculations was outlined in Ref. 9 and discussed in detail in Ref. 12. The exact calculation is based on the geometry shown in Fig. 1. The duct is cylindrical with acoustic treatment on the walls and the steady flow contains sheared flow near the walls. The sheared flow profile is the standard 1/7th power profile to a distance δ from the wall. A linear profile is pieced in near the wall. Only inlet conditions (negative Mach number) are considered with the sound propagation being opposed by the steady flow. The shear layer is uniform in the axial direction and no acoustic reflections are considered. The calculation procedure uses the classical plug flow Bessel function solutions in the duct interior matched to a Runge-Kutta integration through the boundary layer.

Optimum Wall Impedance Definition

The liner optimum acoustic impedance for single mode sound progagation is defined exactly as presented in Ref. 9. Figure 2 illustrates the concept of the optimum impedance for a single mode. The attenuation coefficient (σ) and the propagation coefficient (τ) are components of the complex axial wave number where the acoustic pressure varies as $\exp(\omega/c(\sigma + i\tau)x)$. Note that contours of constant damping (the solid curves) are closed curves in the wall impedance plane. As the attenuation coefficient is increased in value these contours shrink in size and ultimately converge to a point designated by a plus sign. Further increases in damping produce curves which are not closed in the vicinity of this point and in fact represent larger contours associated with the next higher radial mode. This limiting point in Fig. 2 thus represents the impedance with maximum damping for the particular mode under consideration, and this point is designated as the optimum wall impedance for the mode. The associated value of the attenuation coefficient is not considered here but can be found in Refs. 2, 8, and 12. Similar procedures for defining optimum impedance have been published[13-16] in the literature.

Mode Cut-Off Ratio

The definition of mode cut-off ratio is the same as that used in Ref. 9. This can be expressed as,

$$\xi = \frac{\pi\eta}{R\sqrt{(1 - M_o^2)\cos 2\psi}} \qquad (1)$$

where

$$\eta = \frac{fD}{c} \qquad (2)$$

is the frequency parameter and the complex eigenvalue for the mode is given by,

$$\alpha = Re^{i\varphi} \qquad (3)$$

For a hardwall duct equation (1) reduces to the more familiar cut-off ratio expression of Ref. 17. When a spinning mode is highly propagating (ξ large) the acoustic wave motion is mainly in the axial direction, while near cut-off ($\xi \sim 1$) the wave motion is mainly transverse or circumferential.

Correlation of Optimum Impedance

The starting point for the optimum impedance correlation is an equation derived in Ref 12. This equation in turn was derived from the thin boundary layer theory of Ref. 18. The expression is,

$$\zeta = \zeta_m + i\chi_m = \frac{(1 + \epsilon)\zeta_o}{1 - iFG\zeta_o} \qquad (4)$$

where ζ is the optimum wall impedance with the boundary layer refraction considered, ζ_o is the more simply calculated optimum impedance for plug flow (no boundary layer), ϵ is the nondimensional boundary layer thickness, and F in it's simpliest form from Ref. 12 is,

$$F = \frac{\pi\epsilon\eta M_o}{4} \qquad (5)$$

The term G in the denominator of equation (1) was not present in the equation from Ref. 12 and has been inserted for additional empirical corrections to be made in this study. A similar procedure was used in Refs. 8 and 9 to provide an empirical correction to make equation (1) valid down to cut-off ($\xi = 1$), but the term comparable to G was considered to be only a function of cut-off ratio. We will find here that G must also be a function of Mach number (M_o), frequency parameter (η), and boundary layer thickness (ϵ) when a broader parameter range in the exact propagation solution is considered.

Optimum Impedance Without a Boundary Layer

The first step in developing the correlation equation (4) is to generate an expression for the optimum acoustic impedance for the slug flow case which is a function of cut-off ratio. An expression for this optimum impedance is available[10] as,

$$\zeta_o = \theta_{mo} + iX_{mo} = \eta Q^2 (B_\theta - iB_\chi) \qquad (6)$$

where

$$B_\theta \approx \frac{1.15}{\mu + 0.78\, m^{2/3} \mu^{1/4}} \qquad (7)$$

$$B_\chi \approx \frac{0.92}{\mu^2 + 3.17\, \mu m^{2/3}} \qquad (8)$$

and

$$Q = 1 + iM_o(\sigma + i\tau) = \frac{1 - M_o\sqrt{1 - (1 - M_o^2)(\alpha/\pi\eta)^2}}{1 - M_o^2} \qquad (9)$$

Equations (7) and (8) are correlations presented in Ref. 10 and Q^2 is the usual impedance multiplier occurring due to the continuity of displacement boundary condition used at the wall with slip flow.

The terms B_θ, B_χ, and Q must be converted to functions of mode cut-off ratio. This will be done by introducing the eigenvalue into the expressions for B_θ and B_χ such that cut-off ratio may be reinserted. The denominators of equations (7) and (8) are roughly proportional to eigenvalue and eigenvalue squared, respectively, as shown by the curve fits in Fig. 3. Note that Fig. 3 is plotted for $M_o = 0$ in which case $Q = 1$, and from equation (6) $\theta_{mo}/\eta = B_\theta$, and $X_{mo}/\eta = -B_\chi$. The plotted points for $m = 1$, 7, and 20 use $\mu = 1$, 2, 5, and 10 while for $m = 0$ and 50, only $\mu = 1$ was available. By using the curve fits of Fig. 3 and the cut-off ratio definition of equation (1), equation (6) can be written as,

$$\zeta_o \approx \xi Q^2 \sqrt{1 - M_o^2}\left[1 - \frac{i0.84\xi}{\eta}\sqrt{1 - M_o^2}\right] \qquad (10)$$

The quantity Q given by equation (9) must now be expressed as a function of cut-off ratio. Using equations (1) and (3), equation (9) can be expressed as,

$$Q = \frac{1 - M_o\sqrt{1 - \frac{1}{\xi^2}\left(1 + i\,\frac{\sin 2\varphi}{\cos 2\varphi}\right)}}{1 - M_o^2} \qquad (11)$$

The quantity $\sin 2\varphi/\cos 2\varphi$ is still a function of the particular mode under consideration, but it is generally quite small compared to one. Rather than discard this quantity completely an average value based on many modes was calculated. Exact calculations of optimum impedance were compared to equation (10) for modes near cut-off and the phase angle of the second quantity in the radical of equation (11) was estimated. Equation (10) was used since it was anticipated that $\sigma \to 0$ in equation (4) for $\xi \approx 1$ and thus $\zeta \approx \zeta_o$. This average phase angle was found to be twelve degrees (thus $\varphi \approx 6^o$) and equation (11) can be expressed as,

$$Q \approx \frac{1 - M_o\sqrt{1 - e^{i\pi/15/\xi^2}}}{1 - M_o^2} \qquad (12)$$

With this value of Q inserted into equation (10) the optimum impedance correlation is seen to contain modal information only in the form of mode cut-off ratio.

Optimum Impedance With a Boundary Layer

With ζ_o expressed in terms of cut-off ratio alone the function G in equation (4) can now be correlated as a function of cut-off ratio. A multitude of exact calculations of optimum impedance were made using the calculation procedure as outlined in a previous section (Sound Propagation Model). These calculations included many modes from the first propagating spinning mode ($m = 1$, $\mu = 1$) to the highest lobe number which would propagate. A wide range of frequency parameters ($\eta = 5$ to 30), Mach numbers ($M_o = -0.1$ to -0.7), and boundary layer thickness ($\epsilon = 0.005$ to 0.1) were considered. The exact values of optimum impedance were compared to equation (4) and the value of the function G was calculated to obtain equality. The amplitude and phase of G were then correlated with the input parameters to obtain the following correlations. The amplitude of G can be expressed as,

$$|G| \approx \frac{1.1\, e^{-5.41\left(\frac{1 - M_o^2}{\xi}\right)^3}}{1 + 1.5\, F^2} \qquad (13)$$

and the phase as

$$\varphi_G \approx \frac{50}{\xi} - \Delta\varphi_G \qquad (14)$$

where for $|M_o| < 0.5$

$$\Delta\varphi_G \approx \frac{80}{\eta^2 \epsilon |M_o| \xi} \qquad (15)$$

and for $|M_o| > 0.5$

$$\Delta\varphi_G \approx \frac{640\, M_o^2}{\eta^2 \epsilon \xi} \qquad (16)$$

Note that φ_G is expressed in degrees.
Near cut-off the exponential in equation (13) is very small and $G \approx 0$ and $\zeta \approx \zeta_o$. Note that ζ_o (derived for plug flow) does not contain boundary layer thickness, and thus near cut-off the optimum impedance is not a function of boundary layer thickness.

Summary of the Use of the Correlating Equations

The procedure for using the correlating equations will be summarized in this section. First the method of calculation for generating the locus of optimum impedance versus cut-off ratio is presented. This procedure would be followed in an engine inlet design if multimodal noise excitation is considered.

The input parameters η, M_o, and ϵ are determined from the sound frequency, duct size, steady flow rate, and an estimate of the boundary layer thickness. A cut-off ratio is selected for calculation and the complex impedance ζ_o is calculated using equations (10) and (12). The magnitude and phase of the function G are calculated using equations (13), (14), and (5) along with equation (15) or (16) depending upon the magnitude of the Mach number. The two complex quantities ζ_o and G are used in equation (4) (again using equation (5)) to calculate the optimum acoustic impedance components θ_m (resistance) and χ_m (reactance). Another value of cut-off ratio is then selected and the procedure is repeated.

If the optimum impedance of a single mode is to be estimated, the cut-off ratio must be first calculated from equation (1) using the mode eigenvalue at the optimum. The eigenvalue can be calculated from correlations given in Ref. 10 which are repeated here for convenience. The eigenvalue amplitude is,

$$R_{m,\mu} \approx R_{m,1} + (\mu - 1)\pi + 0.076\, m \sqrt{\mu - 1} \qquad (17)$$

where

$$R_{m,1} \approx m + 2.247\, m^{1/3} + 1.521\, m^{-1/3} \qquad (18)$$

The eigenvalue phase is,

$$\varphi_{m,\mu} \approx \varphi_{m,1}\, e^{\frac{-(\mu - 1)}{2(\sqrt{\mu} + m/7)}} \qquad (19)$$

where

$$\varphi_{m,1} \approx \frac{35.15}{(m + 2)^{0.6}} \qquad (20)$$

Equation (18) is valid for $m \neq 0$. If $m = 0$, use $R_{0,1} = 3.278$. These correlations were derived from exact calculations of the optimum eigenvalues for $m = 1$ to 20 and $\mu = 1$ to 10. After the cut-off ratio is calculated the procedure in the first part of this section is followed. Some caution should be exercised when using equation (4) for single mode optimum impedances. As will be shown in a later section, for large lobe numbers (m) and small radial orders (μ) equation (4) must be considered as only an approximation to the exact optimum.

Comparison of Correlation with Exact Calculations

Three input parameters will be varied to illustrate the accuracy of the optimum impedance correlation. These are the frequency parameter (η), steady flow Mach number (M_o) and the boundary layer thickness (ϵ). A base case of $\eta = 15$, $M_o = -0.4$, and $\epsilon = 0.05$ will be used with one parameter at a time being varied from this base.

Figures 4 and 5 compare the correlation with exact calculations for the resistance and reactance, respectively, when boundary layer thickness is varied. The correlation is shown by the curves and the exact calculations are represented by the various symbols with each point being an individual mode optimum calculation. Note that not all modes are shown and that a roughly geometric progression on lobe (m) and radial (μ) number was used to reduce computer time. For example, $m = 1, 2, 3, 5, 9, 16, 30$, and 56, and $\mu = 1, 2, 3, 4, 6, 9, 14$, and 22 were calculated.

From Figs. 4 and 5 it is apparent that the correlation agrees very well with the exact optimum impedance calculations over a wide range of boundary layer thickness. A small error in the resistance correlation occurs at high cut-off ratios and thick boundary layers. A small error is also apparent in the reactance correlation for the thinnest boundary layer. However, in the region of greatest interest, near cut-off through moderate cut-off ratios, the correlation provides excellent results. Note that near cut-off ($\xi = 1$) there is no effect of the boundary layer thickness upon optimum resistance and only a very small effect upon the optimum reactance. This is physically reasonable since at cut-off the wave travel is all circumferential and no velocity gradient occurs in this direction to cause any refraction.

Figures 6 and 7 compare the resistance and reactance correlations with exact calculations for variations of frequency parameter while Figs. 8 and 9 consider variations in Mach number. Again the agreement is seen to be excellent. Some deviations in the resistance correlation occurs at high cut-off ratios and high Mach numbers ($M_o = -0.5$ and -0.7 in Fig. 8). Note, however, that where these errors occur the values of resistance are extremely small and would probably not represent a realistic design case.

It is interesting to note that the correlation follows the exact calculation trends below cut-off ($\xi < 1$) even though the correlation was developed by using exact calculations only down to about $\xi \approx 1.1$. The double inflections of the reactance trends apparent in Figs. 5, 7, and 9 are even preserved by the approximate equation.

Limitations of the Optimum Impedance Correlation

As with any empirical correlation, there is some danger in extrapolating beyond the data base from which the correlation was derived. The base case as previously mentioned used $\eta = 15$, $M_o = -0.4$, and $\epsilon = 0.05$ which were considered as typical values for a turbofan engine inlet. The correlation was developed for a three variable grid of points through this base point and the correlation was shown to be reliable along these grid lines. Some calculations off of these grid lines were made to check the correlation and these are shown in Figs. 10 and 11 for the resistance and reactance respectively. For $\eta = 5$, $M_o = -0.2$, and $\epsilon = 0.05$ the correlation is seen to hold quite well. For $\eta = 20$, $M_o = 0.7$, and $\epsilon = 0.1$ the reactance correlation is seen to be good (Fig. 11) but the resistance correlation (Fig. 10) is seen to be predicted somewhat low. This is a case of extreme refraction in the boundary layer giving a rapid fall-off of resistance above cut-off and the correlation somewhat over predicts this effect. For a low frequency, high Mach number, thick boundary layer case

(η = 5, M_o = -0.7, ϵ = 0.10) both the resistance and reactance correlations are seen to deviate substantially from the exact calculations. The resistance is over-predicted for moderate to high cut-off ratios while the reactance is under-predicted for low to moderate cut-off ratios.

It is thus suggested that extrapolations away from the data base can be made for low Mach numbers, but considerable error may occur for high Mach numbers, especially for low frequencies.

A second limitation of the optimum impedance correlation occurs at the lower radial orders (low μ) of the high lobe number (m) modes. This problem was apparent for the zero Mach number results of Fig. 3 and was also pointed out in Ref. 9. This limitation would have been evident in all of the calculations made for generating Figs. 4 to 11 but these cases were omitted to avoid obscuring the points to be made in these figures. In order to illustrate the error in the correlation for these higher lobe number modes. All of the exact calculations are included in Figs. 12 and 13 for the optimum resistance and reactance respectively. Progressively higher radial modes, for a given lobe number, can be identified by a decreasing cut-off ratio. In Fig. 12 some deviation from the correlation is seen for the first radial of the nine lobed mode, while the second, third, and higher radials are seen to be approaching the correlation. As the lobe number is increased to 16 and 30 the error in using the correlation for the first radial mode is seen to increase. Again the higher radial orders are seen to approach the correlation. The same behavior holds for the optimum reactance shown in Fig. 13. The error for the first radial mode is significant for m = 16 and increases substantially for m = 30. The errors can be interpreted as an inaccurate representation of the low radial, high lobe number modes by cut-off ratio alone. It is the author's opinion that these small errors for a few modes will not significantly affect the results in a multimodal situation. However, if this correlation is used for single mode estimates of optimum impedance one should be aware of the error for the high lobe number modes.

Concluding Remarks

A semi-empirical correlation for the optimum acoustic impedance for spinning modes in a circular duct has been presented. An engine inlet flow condition with a boundary layer at the wall and a uniform velocity profile in the central core was considered. The correlation is part of an acoustic liner design method being developed for multimodal sound propagation from an aircraft engine through the acoustically lined inlet duct and out into the far-field. The philosophy of this approach was summarized in Ref. 8 and the far-field radiation concepts were reported in Ref. 11. The key to this approach is the distribution of acoustic power as a function of mode cut-off ratio. The elements yet to be developed are the power distribution shifts caused by modal scattering in the acoustic liner and possibly at the duct termination.

The optimum acoustic impedance equation presented here represents an improvement upon earlier published forms. A wide range of input parameters were considered here in constrast to that used for the equation's earlier form. The correlation can be used to quickly estimate optimum impedance and eliminates the elaborate computer programs and considerable computer running time needed for exact calculations.

The use of the correlation for design estimates requires some knowledge of the modal properties of the noise source. Rough estimates of the gross modal properties can be made. For example, in a stationary engine or fan test installation a considerable amount of the acoustic power occurs in the modes near cut-off. An efficient liner might be expected using a near cut-off liner design. For a flight situation the noise often consists of multiple pure tones and blade passage frequency. The dominant modes expected for the multiple pure tones (shock noise) can be estimated perhaps from rotor locked mode considerations. These modes will most likely be closed to cut-off. The modes for blade the passage frequency tones and their associated cut-off ratios can be estimated from rotor-stator interaction theory (Ref. 17).

References

1. Yurkovich, R., "Attenuation of Acoustic Modes in Circular and Annular Ducts in the Presence of Uniform Flow," AIAA Paper 74-552, June 1974.

2. Rice, Edward J., "Spinning Mode Sound Propagation in Ducts with Acoustic Treatment," NASA TN D-7913, May 1975.

3. Motsinger, R. E., Kraft, R. E., and Zwick, J. W., "Design of Optimum Acoustic Treatment for Rectangular Ducts with Flow," ASME Paper 76 GT-113, Mar. 1976.

4. Ko, S. H., "Theoretical Prediction of Sound Attenuation in Acoustically Lined Annular Ducts in the Presence of Uniform Flow and Shear Flow," Journal of the Acoustical Society of America, vol. 54, Dec. 1973, pp. 1592-1606.

5. Yurkovich, R., "Attenuation of Acoustic Modes in Circular and Annular Ducts in the Presence of Sheared Flow," AIAA Paper 75-131, Jan. 1975.

6. Motzinger, R. E., Kraft, R. E., Zwick, J. W., and Vukelich, S. I., "Optimization of Suppression for Two-Element Treatment Liners for Turbomachinery Exhaust Ducts," General Electric Co., Cincinnati, Ohio, R76AEG256, Apr. 1976; NASA CR-134997, 1976.

7. Pickett, G. F., Sofrin, T. G., and Wells, R. A., "Method of Fan Sound Mode Structure Determination," NASA CR-135293, 1977.

8. Rice, E. J., "Inlet Noise Suppressor Design Method Based Upon the Distribution of Acoustic Power with Mode Cutoff Ratio," Advances in Engineering Science, Volume 3, NASA CP-2001-Vol-3, 1976, p. 883.

9. Rice, E. J., "Acoustic Liner Optimum Impedance for Spinning Modes with Mode Cut-Off Ratio as the Design Criterion," AIAA Paper 76-516, July 1976.

10. Rice, E. J., "Attenuation of Sound in Ducts with Acoustic Treatment -- A Generalized Approximate Equation," NASA TM X-71830, 1975.

11. Rice, E. J., "Multimodal Far-Field Acoustic Radiation Pattern -- An Approximate Equation," AIAA Paper No. 77-1281, Oct. 1977, also NASA TM 73721.

12. Rice, E. J., "Spinning Mode Sound Propagation in Ducts with Acoustic Treatment and Sheared Flow," AIAA Paper 75-519, Mar. 1975; also NASA TM X-71672.

13. Cremer, Von Lothar, "Theorie der Luftschall - Dämpflung im Rechteckkanal nit Schluckender Wand und das Sich Dabei Ergebende Hochste Dampfungsmass (Theory of Sound Attenuation in a Rectangular Duct with an Absorbing Wall and the Resultant Maximum Coefficient)," Acoustica, Vol. 3, no. 2, 1953, pp. 249-263.

14. Tester, B. J., "The Optimization of Modal Sound Attenuation in Ducts, in the Absence of Mean Flow," Journal of Sound and Vibration, Vol. 27, Apr. 1973, pp. 477-513.

15. Zorumski, W. E. and Mason, J. P., "Multiple Eigenvalues of Sound-Absorbing Circular and Annular Ducts," Journal of the Acoustical Society of America, Vol. 55, June 1974, pp. 1158-1165.

16. Schauer, J. J. and Hoffman, E. P., "Optimum Duct Wall Impedance-Shear Sensitivity in Acoustic Ducts," AIAA Paper 75-129, Jan. 1975.

17. Sofrin, T. G. and McCann, J. F., "Pratt and Whitney Experience in Compressor-Noise Reduction," Preprint 2D2, Nov. 1966, Acoustical Society of America, 72nd. Meeting, Los Angeles, California.

18. Eversman, W. and Beckemeyer, R. J., "Transmission of Sound in Ducts with Thin Shear Layers-Convergence to the Uniform Flow Case," Journal of the Acoustical Society of America, Vol. 52, July 1972, pt. 2, pp. 216-220.

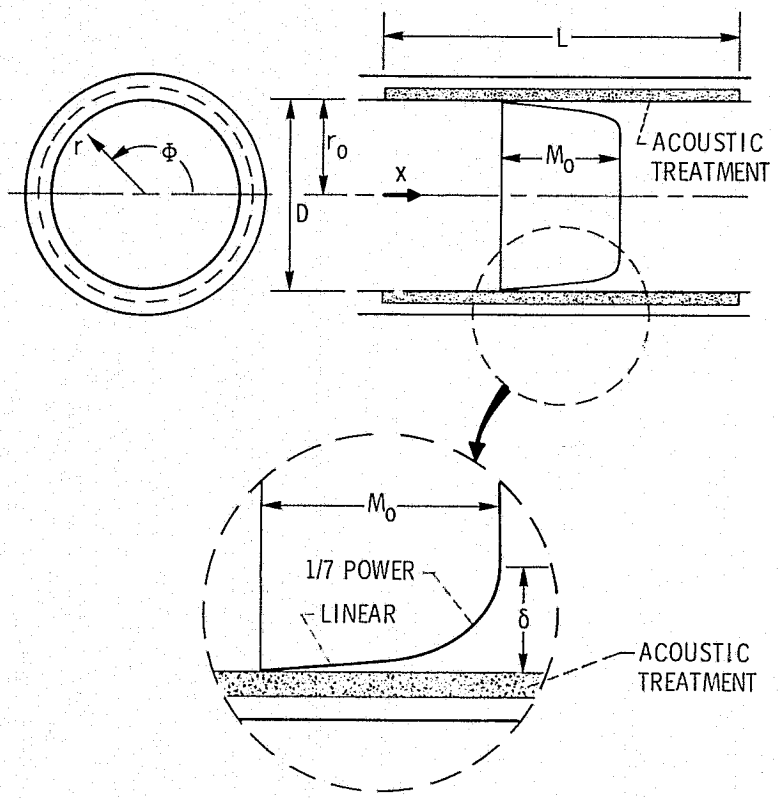

Figure 1. - Geometry and steady-flow velocity profile.

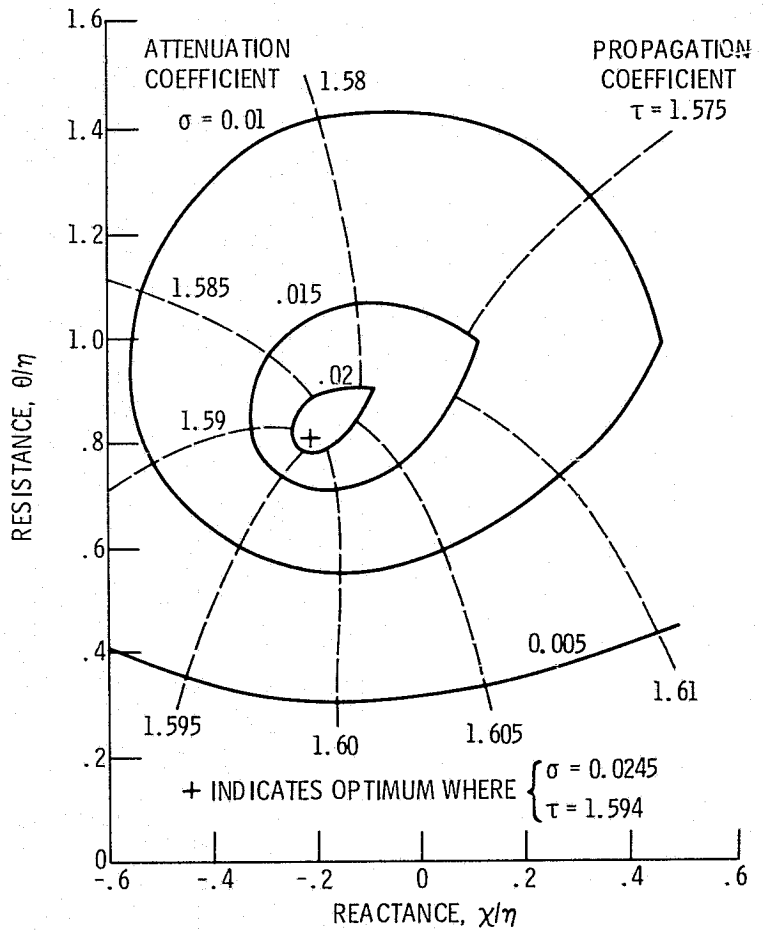

Figure 2. - Constant attenuation and propagation contours for the least attenuated spinning mode using displacement boundary condition. Inlet Mach number, $M_0 = -0.4$; lobe number, m = 7; frequency parameter, $\eta = 10$; boundary layer thickness, $\delta/r_0 = 0$.

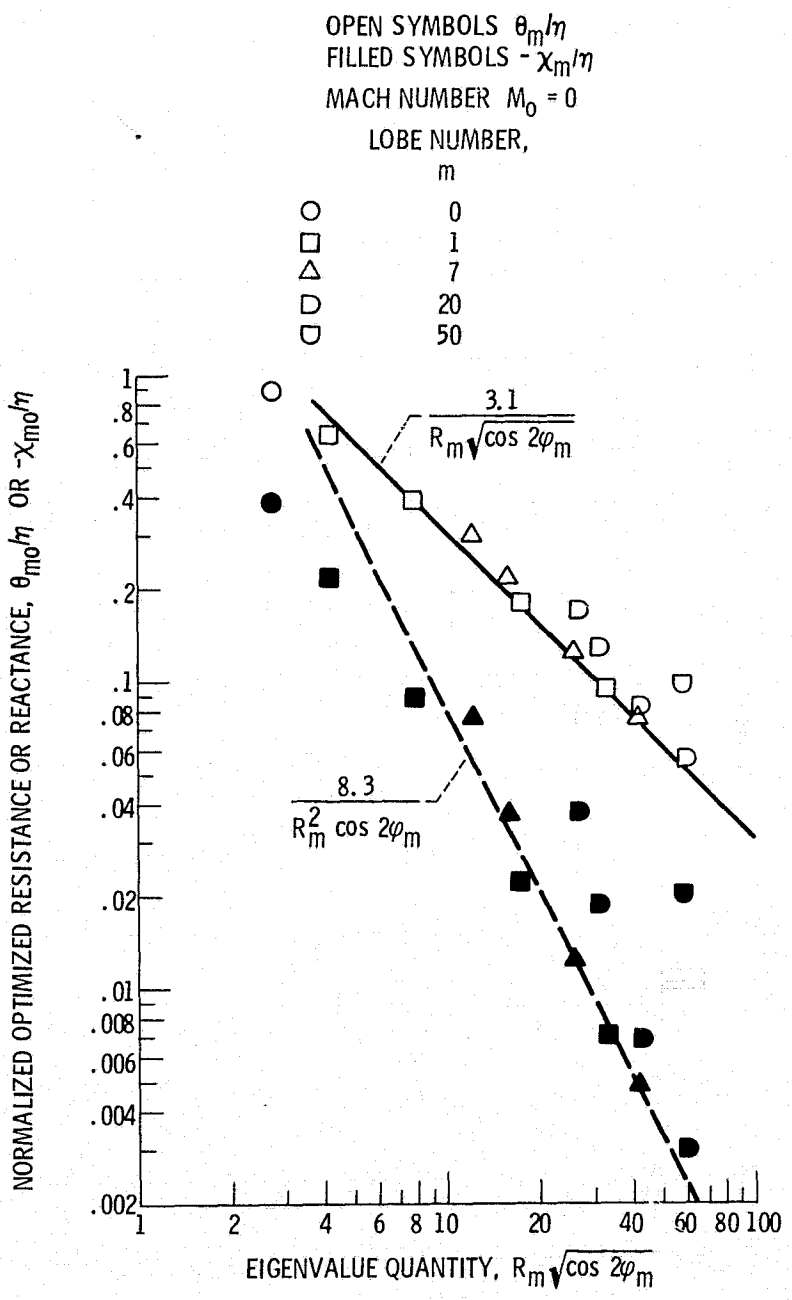

Figure 3. - Correlation of optimum resistance and reactance with mode eigenvalue.

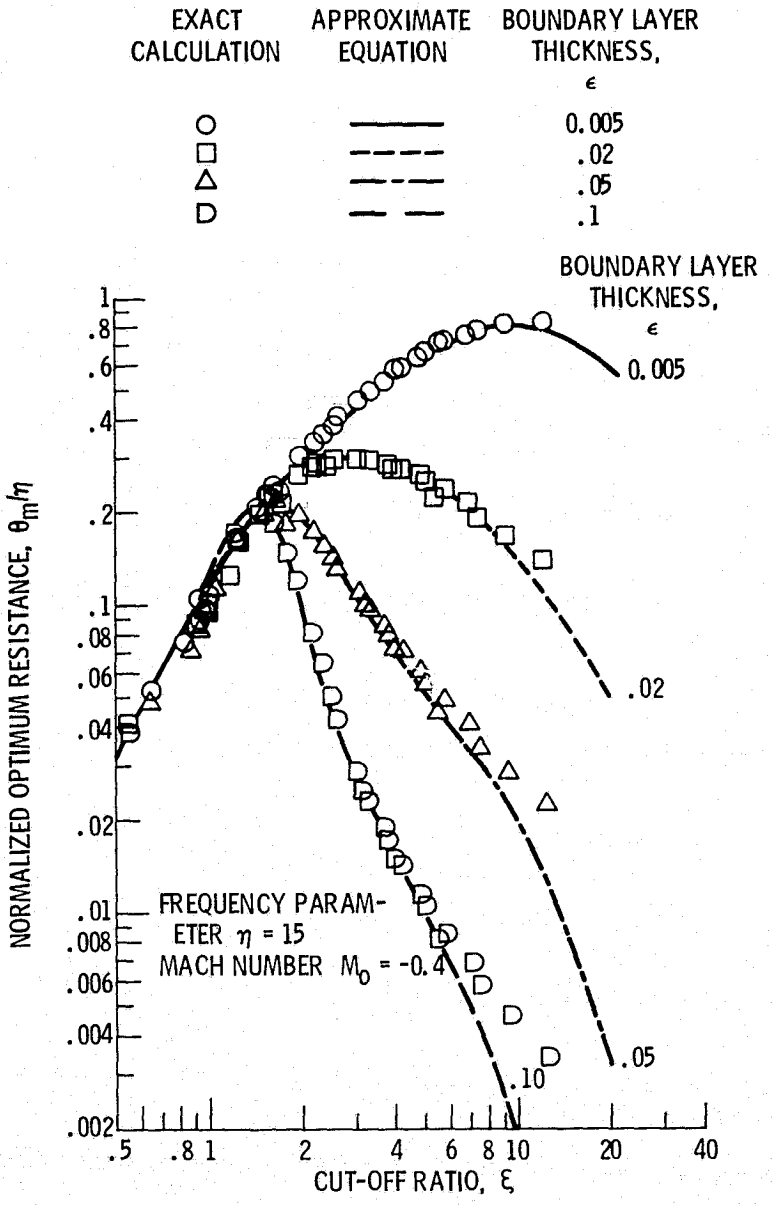

Figure 4. - Comparison of correlating equation with exact calculations of optimum resistance for variations in boundary layer thickness.

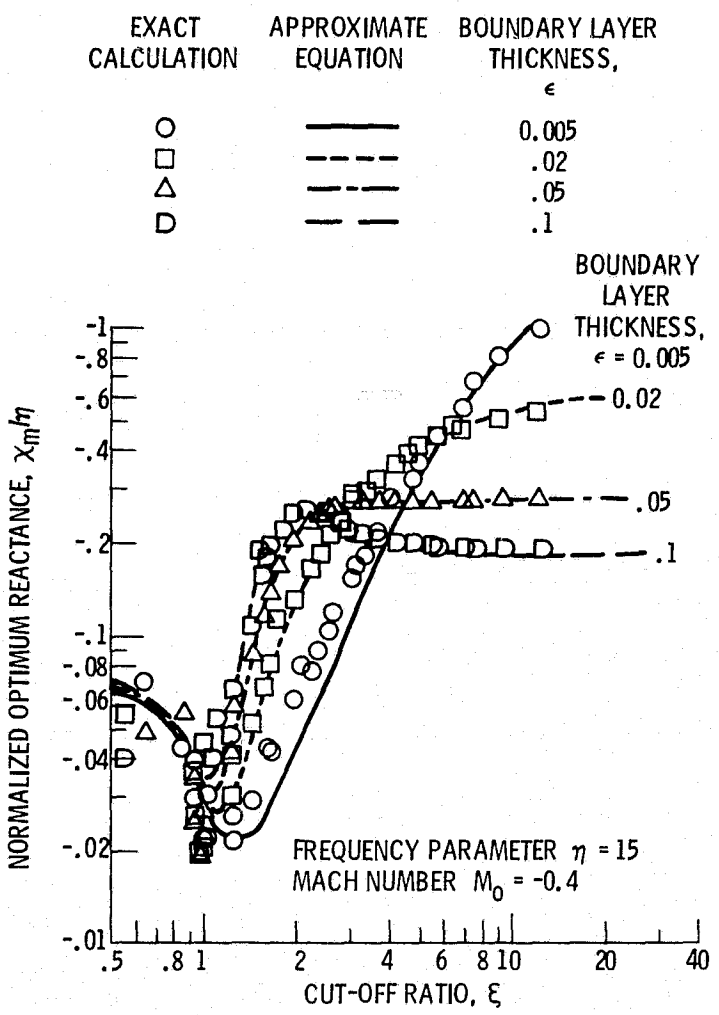

Figure 5. - Comparison of correlating equation with exact calculations of optimum reactance for variations in boundary layer thickness.

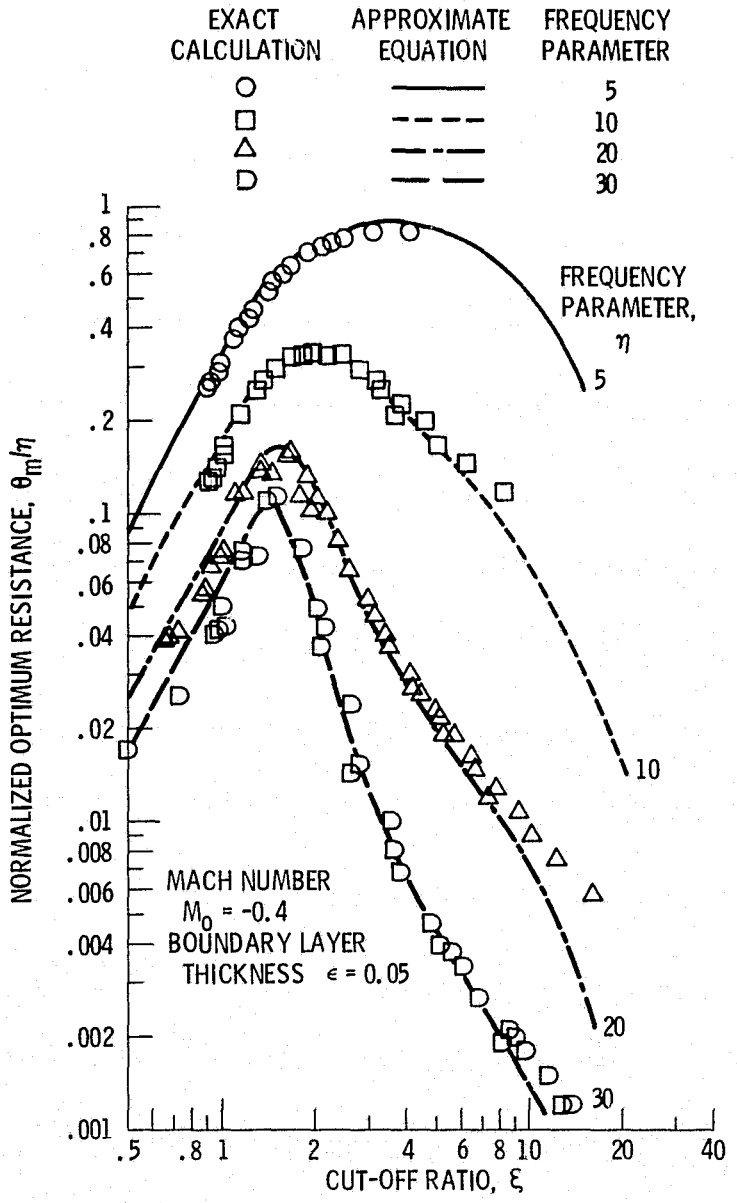

Figure 6. - Comparison of correlating equation with exact calculations of optimum resistance for variations of frequency parameter.

E-9451

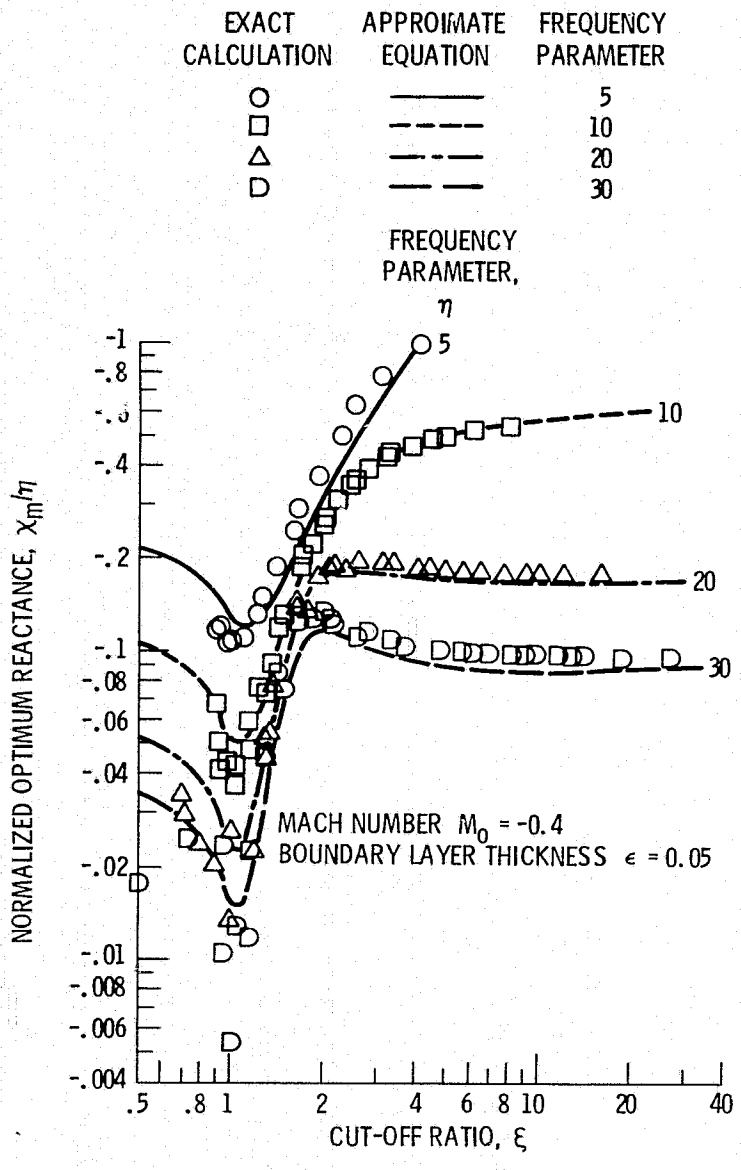

Figure 7. - Comparison of correlating equation with exact calculations of optimum reactance for variations of frequency parameter.

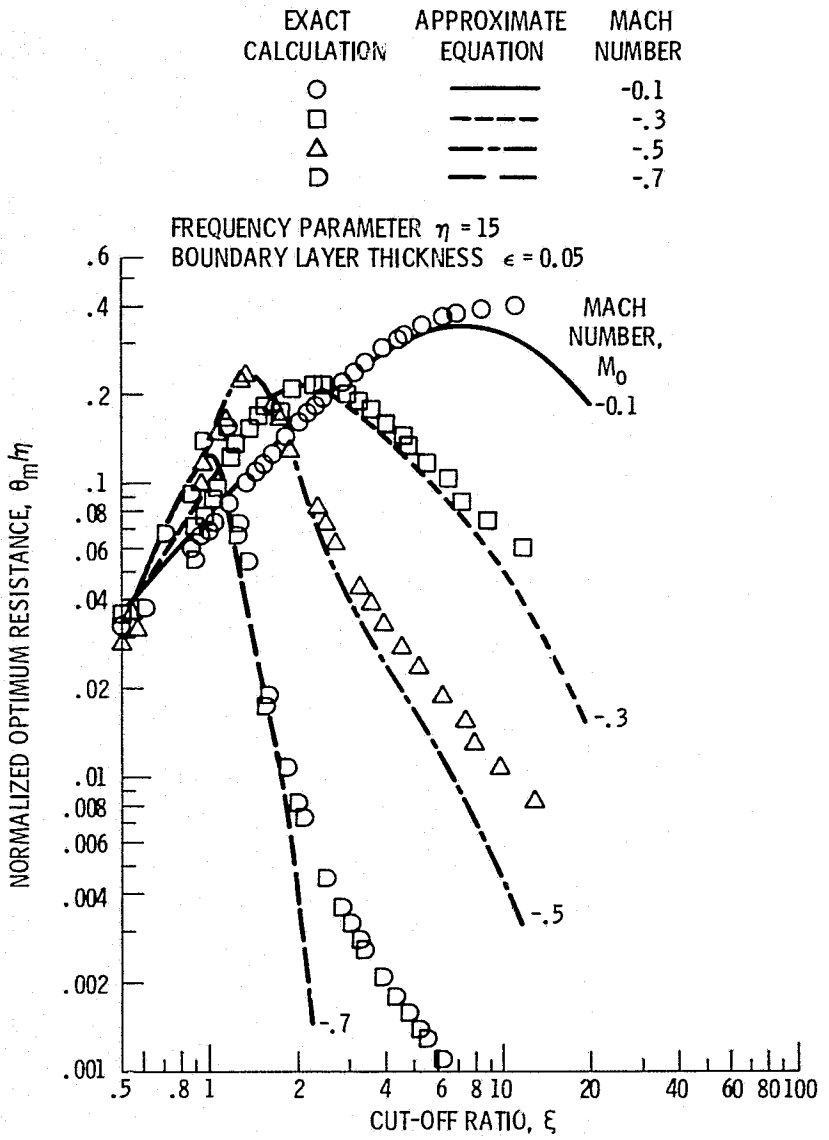

Figure 8. - Comparison of correlating equation with exact calculations of optimum resistance for variations in steady flow Mach number.

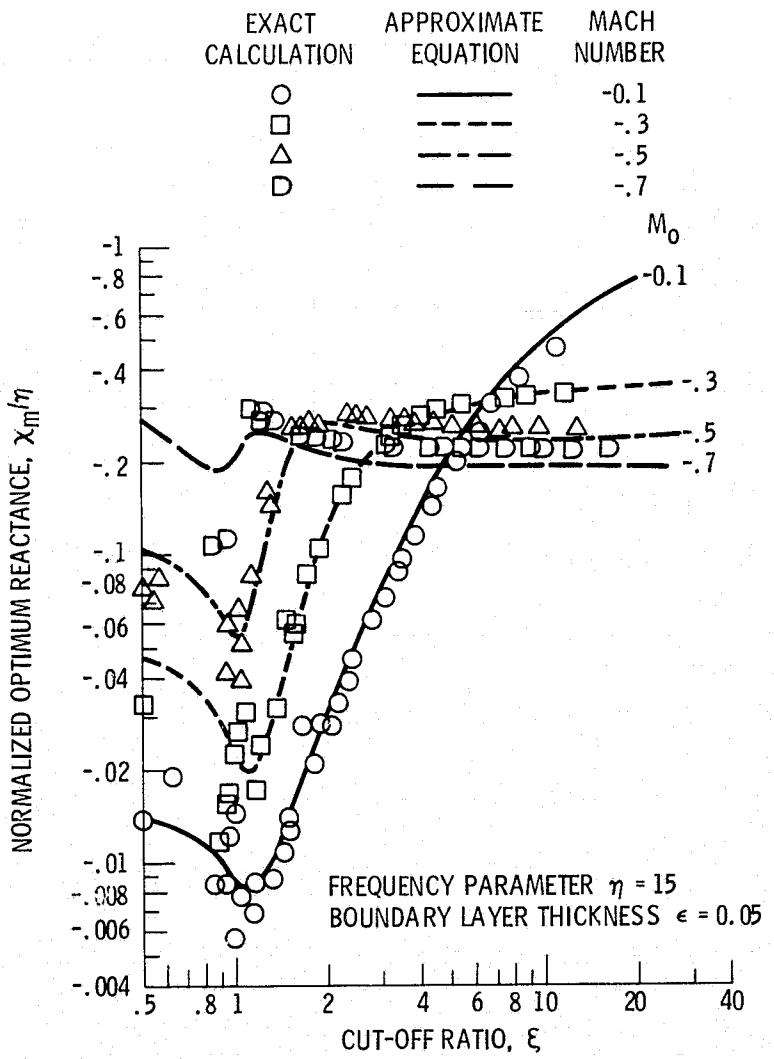

Figure 9. - Comparison of correlating equation with exact calculations of optimum reactance for variations in steady flow Mach number.

EXACT CALCULATION	APPROXIMATE EQUATION	FREQUENCY PARAMETER, η	MACH NUMBER, M_0	BOUNDARY LAYER THICKNESS, ϵ
○	———	5	-0.2	0.05
□	- - -	5	-.7	.10
△	— - —	20	-.7	.05

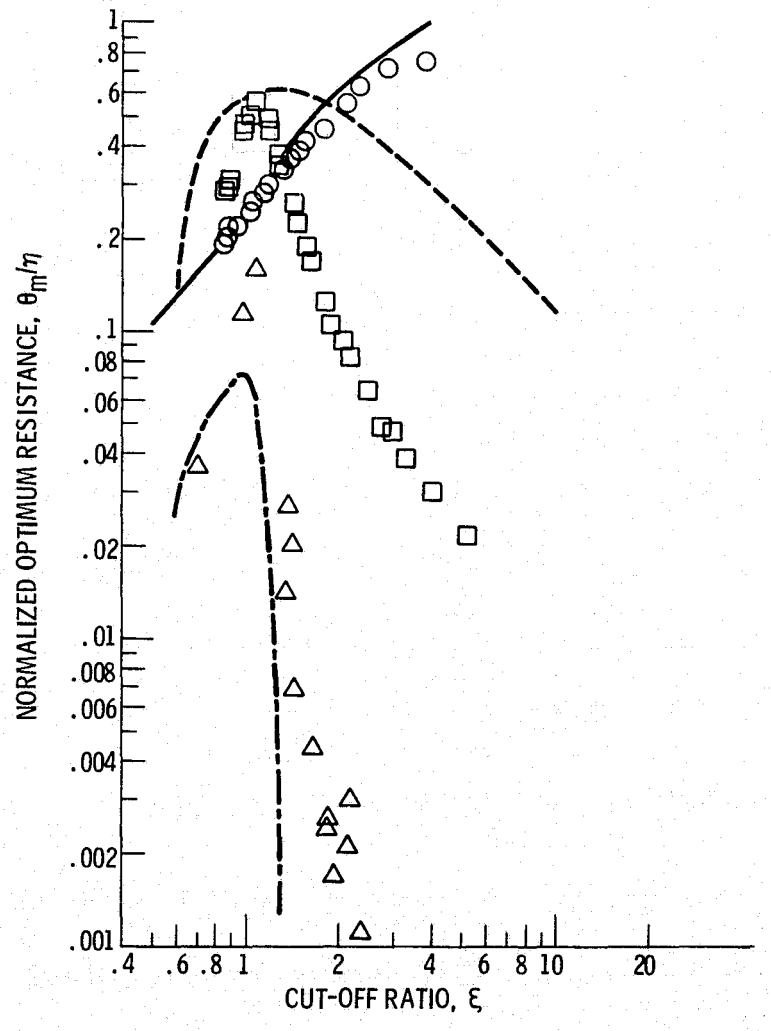

Figure 10. - Comparison of exact calculations of optimum resistance with extrapolated correlating equation.

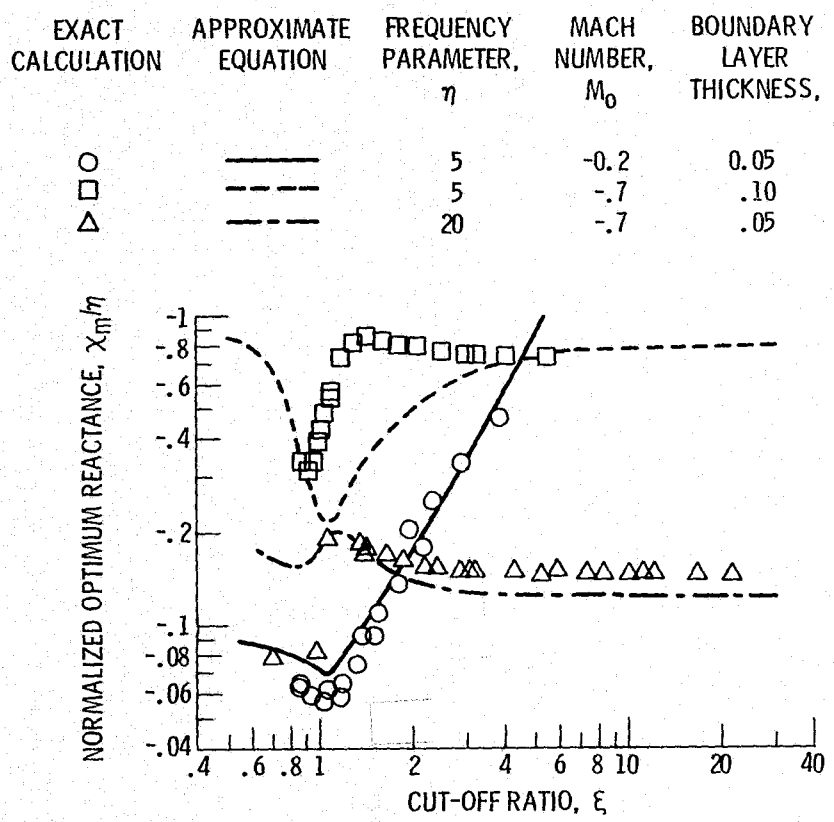

Figure 11. - Comparison of exact calculations of optimum reactance with extrapolated correlating equation.

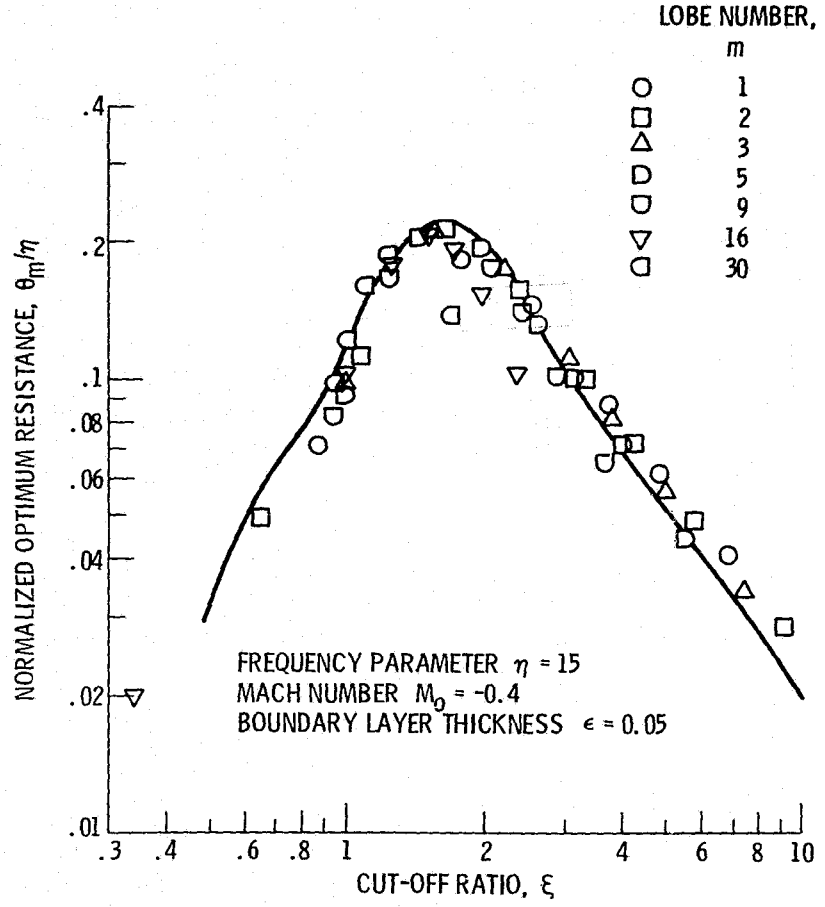

Figure 12. - Deviation of high lobe number modes from the acoustic resistance correlation.

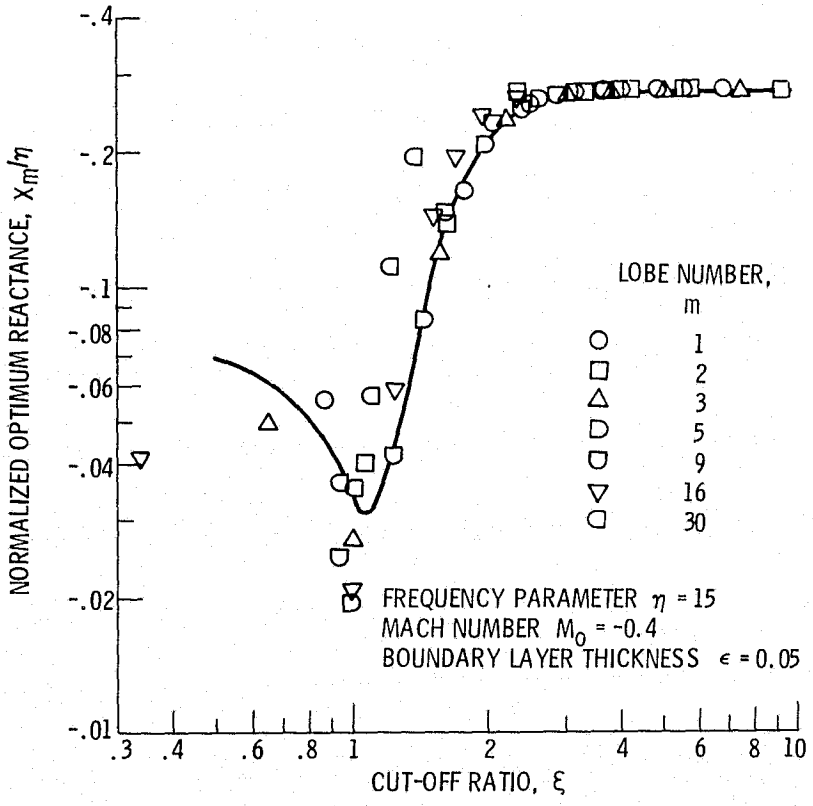

Figure 13. - Deviation of high lobe number modes from the acoustic reactance correlation.

NASA-Lewis-